Journal of Inclusion Phenomena **3**, 317–333. 0167–7861/85.15.

Stereospecific Reactions and Interactions in Tri-*ortho*-thymotide Clathrates★

R. ARAD YELLIN, B. S. GREEN
Department of Structural Chemistry, Weizmann Institute of Science, 76100 Rehovot, Israel

M. KNOSSOW, N. RYSANEK and G. TSOUCARIS★★
Laboratoire de Physique, ER 180, TOUR B, Centre Pharmaceutique, 92290 Chatenay-Malabry, France

(Received: 22 January 1985)

Abstract. The emphasis in this paper is on the interpretation of physicochemical phenomena occurring in tri-*ortho*-thymotide (TOT) clathrates in the light of crystallographic data.

Enantiomeric discrimination of guest included in the cage $P3_121$ clathrates, first suggested by H. M. Powell, has been studied for about twenty guest molecules. Practical applications include preparative resolution and determination of the absolute configuration of guest molecules via TOT clathrates. The observation of similar position and orientation within the cage of stereochemically related guests, provides a clue for the chiral discrimination in terms of crystallographic data. The influence of different factors (guest size, crystallographic disorder, etc.) is analyzed, as well as the difficulties in obtaining a precise assignment of the chirality of host/guest interactions.

TOT clathrates including stilbene and cinnamic acid as guest undergo photoisomerization reactions whose pathway is different from that observed in solution or in the pure guest crystal, due to the different microenvironment around the olefinic molecule.

It is shown that symmetry, as well as crystallographic disorder, is the most important factors governing these phenomena. The analysis of these factors bears similarities with the problems arising in chiral discrimination. In particular, the flexibility of the TOT molecule is probably strongly correlated with the physicochemical phenomena so far studied, as well as with the large variety of crystal forms. The comparison of the TOT molecular configurations in five different crystallographic environments allows a critical discussion on the pertinent molecular parameters which reflect the TOT flexibility.

Key words: TOT, chiral discrimination, stereospecific reactions.

1. Introduction

Although tri-*ortho*-thymotide (TOT) was first prepared in 1865 [1], the TOT clathrates were discovered and first studied in 1952 [2–4]; they are among those which have been the object of thorough studies by a combination of structural investigations and physicochemical experiments. These experiments may involve only van der Waals or residual force host-guest interactions; they include enantiomeric separation, isolation of monomeric carboxylic acids, etc. But they also may involve photochemical and thermochemical reactions of the guest molecules alone or reactions between the cage molecules and the guest. Among studies on other clathrates of comparable scope, we particularly mention those on deoxycholic acid adducts where the occurrence of specific photochemical reactions – in this case between host and guest – necessitates combined chemical and crystallographic investigations [7]. Two main

★ Dedicated to Professor H. M. Powell.
★★ Author for correspondence.

themes of host–guest interaction have been investigated up to now: chiral discrimination and lattice dependant photochemical reactions of the included guest.

In the chirality domain, H. M. Powell [5, 6], after reviewing Pasteur's methods, pointed out that 'New classes of optically active materials arise when a surrounding molecular structure will include a molecule more readily as one enantiomorphous form than as the other'. Two prominent results have been achieved now in this area: *enantiomeric purification of guest* and determination of the *absolute configuration* of TOT, opening up the possibilities of separating and determining the absolute configuration of chemically inert molecules for which the usual techniques are ineffective. In the photochemistry area, the *cis–trans photoequilibrium* of olefin derivatives has been shown to be very dependant on the lattice symmetry, as well as on stereochemical factors.

A common feature of these phenomena is the marked influence of the surrounding host on the guest molecules, resulting in a change of the reaction path, or in general of the guest's behaviour, as compared with the free guest or the free guest in solution. The specificity of host/guest interaction will be the guideline throughout this paper. A new example thereof will be provided in Section 5 concerning the isolation of monomeric species of carboxylic acids. Here, the clathrate formation profoundly modifies the usual intermolecular organization of the guest in solution.

Before describing the results of the physicochemical experiments we deal, in the next section, with two general characteristics of TOT clathrates: *molecular flexibility of the host* and the *variety of crystal forms*. A related topic is the molecular symmetry of TOT; new calculations are performed and the results will be discussed below.

2. Molecular and Crystal Data

At the molecular level, TOT (Figure 1) is quite a flexible molecule existing as two principal conformers: the propeller form (all three carbonyls pointing to one side of the 12-membered central ring) and the helical form (one carbonyl pointing to a side opposite to that of the other two) [8]. In solution, the propeller form is predominant (estimated abundance of 86% at 68 °C in C_2H_5OH); in the clathrates studied so far, only this form is observed. We note however that a related molecule, *N*, *N'*, *N''*-trimethyltrianthranilide, crystallizes in the helical conformation [9]. Both forms, as well as their enantiomorphs, interconvert at room temperature. The

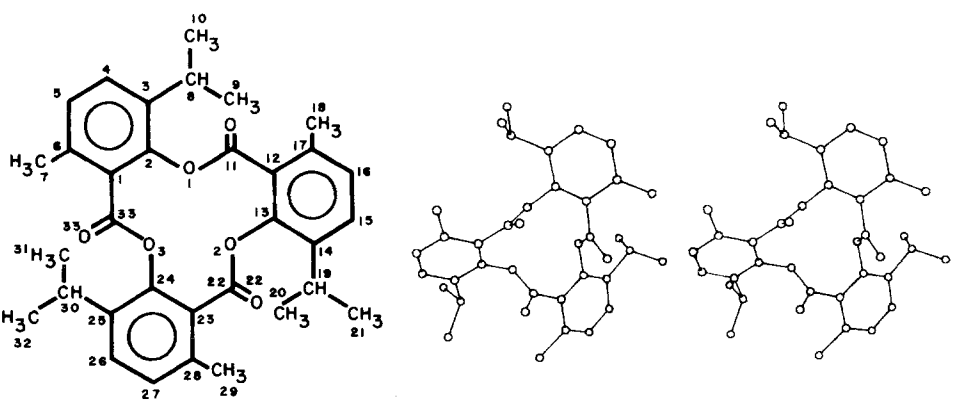

Fig. 1. Structure of the tri-*o*-thymotide (TOT) molecule showing the atomic numbering used in the crystal structure analysis. The stereodrawing on the right illustrates the propeller-like conformation of TOT in the solid.

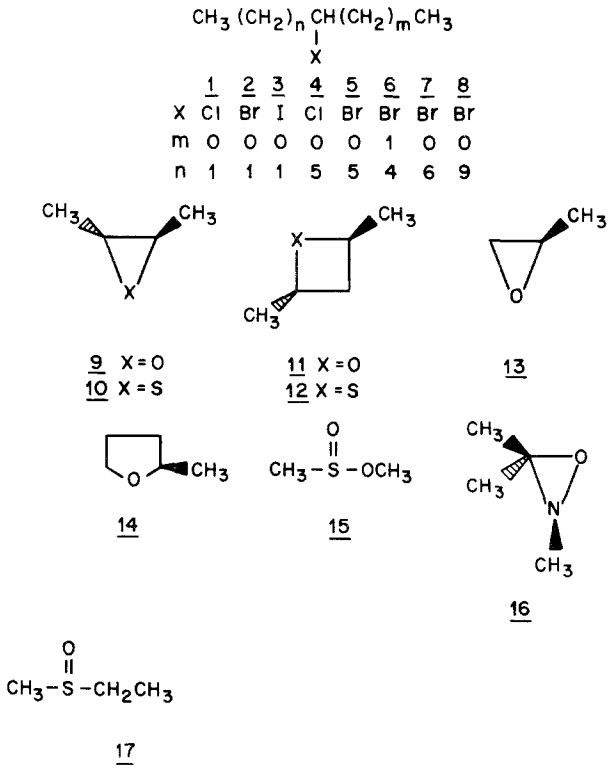

activation energies are about 80–88 kJ, slightly depending on the solvent (the half-life time being ~ 20 min).

At the crystal lattice level, TOT clathrates crystallize in a variety of space groups and display different forms of cavities: cage, quasi-uniform channels, and channels of noticeably variable section.

Three crystal types have been investigated, of space groups $P3_121$, $P6_1$, and $P\bar{1}$. Table Ia includes data for typical representatives of these groups. It has been suggested that the

Table Ia. Crystallographic data of TOT clathrates

	9	*trans*-stilbene	cetyl alcohol
a Å	13.484	11.639	14.308
b Å	13.484	13.027	14.308
c Å	30.44	24.409	29.016
$\alpha°$	90.0	96.05	90.0
$\beta°$	90.0	103.21	90.0
$\gamma°$	120.0	84.81	120.0
Group	$P3_121$	$P\bar{1}$	$P6_1$
z	6	2	6
TOT/guest	2 : 1	2 : 1	6 : 1.3
Form	Cage	Variable section channels	Parallel quasi-uniform channels

$P\bar{1}$ clathrate structure can be visualized as a distorted non-closest hexagonal packing of TOT molecules [17]. Table Ib indicates various guests for which a precise crystal structure determination is available. Within each type, the lattice parameters may vary significantly (up to 0.35 Å).

Table Ib. Guest molecules for which crystal structure determinations have been performed

	Guest	Initial solution	Ref.	Guest	Initial solution	Ref.
$P3_121$	Ethanol	Achiral	[10]	**9**	O.P.[1]	[13]
	Pyridine	Achiral	[11]	**10**	O.P.	[13]
	2	Racemic	[12]	**10**	Racemic	[13]
	2	from 34% O.P. solution	[13]	**17**	Racemic	[14]
$P\bar{1}$	*Trans*-stilbene	Achiral	[16]	Benzene	Achiral	[17]
	Cis-stilbene	Achiral	[16]			
$P6_1$	Cetyl alcohol	Racemic	[10]			

[1] O.P.: Optically pure.

Several other clathrate types are known to exist, but their crystal structures have not been yet determined: $P2_1$ (*meso*-2,3-butanediol carbonate); *Pbca* (fluothane); *Pbcn* (*dl*-2,3-dibromobutane); $C2/c$ (3-bromooctane) [13, 16]. We mention also the channel clathrates of space group $P3_1$, $P2_1$ [4].

An almost constant feature of the clathrates so far studied is the presence of disorder of the guest molecules; it will be the object of a thorough study in the following sections. We note, however, an exception: *trans*-stilbene in $P\bar{1}$.

The factors govering the 'choice' of the crystal form include primarily the size of the guest, and, to a lesser extent, the experimental conditions. For a large variety of molecules, including hydrocarbons, mono and dihalogenoalkanes, ethers, etc. it has been observed that molecules of length less than 9 Å give rise to cavity-type crystals; those of greater length yield a uniform section channel. Larger molecules, e.g. *cis*- or *trans*-stilbene, induce crystallization in a form containing even larger cavities and channels of variable section.

An elegant illustration of the guest's influence on the crystal lattice has been provided by Powell and Lawton [4]: within an isomorphous series of hexagonal channel clathrates, the length of the unit cell axis was shown to be correlated with the length of the included molecule.

In the propeller form, TOT is often quoted as the archetype of organic molecules having C_3 symmetry. It is interesting to inquire about the degree of resemblance of the TOT molecule in various crystalline environments, as well as about the deviations from the ideal C_3 symmetry. Table IIa shows the maximum deviation between three (equivalent by C_3) torsion angles in the 12-membered inner ring. Both independent molecules in the *trans*-stilbene clathrate exhibit the fewest deviations. Table IIb includes torsion angles for three structural types: unsolvated $Pna2_1$, channel $P\bar{1}$, cage $P3_121$. A graphical comparison is also instructive (Figure 2) [10]: most of the continuous lines, which indicate the variations in a given parameter, never cross; i.e. there is a marked element of consistency in the deformations of these molecules. The mean values suggest the 'ideal' C_3 molecule would have the torsion angles indicated in Table IIb. It is not easy to analyse and interpret these data. Here we only note torsion angles that deviate

Table II. Parameters defining the stereochemistry of TOT

Table IIa. Maximum variation of torsion angles (deg.) defining the stereochemistry among the three subunits in the 12-membered central ring of TOT

	I	II	III	IV	V
(a, e, i)	3	2.1	10	13	10
(q, u, s)	4.6	0.7	10	10	10
(b, f, j)	11	7	15	20	25
(l, h, d)	3.5	4.7	32	15	12
(t, r, p)	11.5	9.5	15	25	28
(c, k, g)	6.5	3.4	10	10	8

TOT molecule labelled as follows: I and II, TOT in *trans*-stilbene clathrate; III, TOT in unsolvated TOT (from [10] and [18]); IV, TOT in a channel complex (from [10]); V, TOT in a cage complex (from [11] and [10]).

Dihedral angles labelled as follows: (a, e, i), dihedral angle [O(1), C(2), C(1), C(33)] and its equivalents; (q, u, s), dihedral angle [C(2), C(1), C(33), C(24)] and its equivalents; (b, f, j), dihedral angle [C(2), C(1), C(33), O(3)] and its equivalents; (l, h, d), dihedral angle [C(1), C(2), O(1), C(11)] and its equivalents; (t, r, p), dihedral angle [C(24), C(23), C(22), O(22)] and its equivalents; (c, k, g), dihedral angle [C(2), O(1), C(11), C(12)] and its equivalents.

from the 'ideal' value markedly and quite consistently for all structural types, including the least distorted $P\bar{1}$: b (about 52° instead of 60°); j (ranging from 63° to 77°, instead of 60°); l (ranging from 73 to 82°, instead of 90°); p (132°, instead of 120°); c and k (171° instead of 180°). By contrast, the sequence (e, f, r, q, s, h, i) tends to be closer to the 'ideal' values for most structural types. We note particularly large deviations from C_3 symmetry for the unsolvated form. We recall also that the carbonyl oxygen O(11), involved in the 'distorted' torsion angles t and u, is disordered in $P3_121$ [13,22]. An interesting question is whether the crystallographic data reflect a tendency of part of the molecule to flip over during the interconversion between the propeller and the helical form [10].

In view of a more detailed description of the real molecule, the 'best' 3-fold axis has been determined and the departure from ideal symmetry can be appreciated from data given in Table IIc. The definition of the 3-fold axis C_3 is best achieved by using the most 'rigid' part of the molecule indicated below (n = 10 atoms).

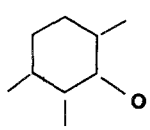

If we denote by α, β, γ the three subunits related by C_3, r_i the actual atomic position, and n the number of atoms in each subunit, the overall pseudo-symmetry is then given by the expression:

$$\sigma = \frac{1}{\sqrt{3}} \sum_{i=1}^{n} \left\{ \frac{|r_i^\alpha - r_i^\beta|^2 + |r_i^\alpha - r_i^\gamma|^2 + |r_i^\beta - r_i^\gamma|^2}{n} \right\}^{1/2}$$

Table IIb. Torsion angles

	I	III	V	Ideal model
i	4	1	−8	
a	1	2	−5	
e	1	−6	+4	0
<>	2	−1	−3	
q	6	−8	−5	
u	2	−9	−25; +15	
s	5	5	0	0
<>	4	−4	−5	
b	52	50	53	
f	63	60	52	
j	63	69	77	60
<>	59	59	60	
l	80	73	82	
h	83	88	91	
d	84	106	94	90
<>	82	89	89	
−*t*	120	112	95; 126	
−*r*	121	123	131	
−*p*	131	133	131	120
<>	124	122	120	
c	171	170	170	
k	172	171	173	
g	178	180	177	180
<>	173	173	173	

I Molecule in *trans*-stilbene [16]
III Unsolvated form [16]
V Cage acetic acid complex [22]. The two values of *u* and *t* in V correspond to the two disorder positions of O(11).

Table IIc. Coordinates of the C_3 axis in the acetic acid clathrate

	x	*y*	*z*
origin	0.3649	0.8813	0.1173
direction of unit vector	−0.0655	−0.0626	−0.0171

$\sigma = 0.42$

The calculated value (for the acetic acid clathrate) of $\sigma = 0.42$ Å denotes a significant, yet quite small, overall deviation from C_3 symmetry. The same calculations including all 39 atoms of the molecule lead to a much larger value: 1.3 Å. The deviation from C_3 symmetry is largely due to one of the methyls of the isopropyl group [C(11)].

Finally, it is interesting to discuss the stability of the TOT atomic coordinates within isomorphous series. After referring to a common coordinate frame, the TOT molecule in space

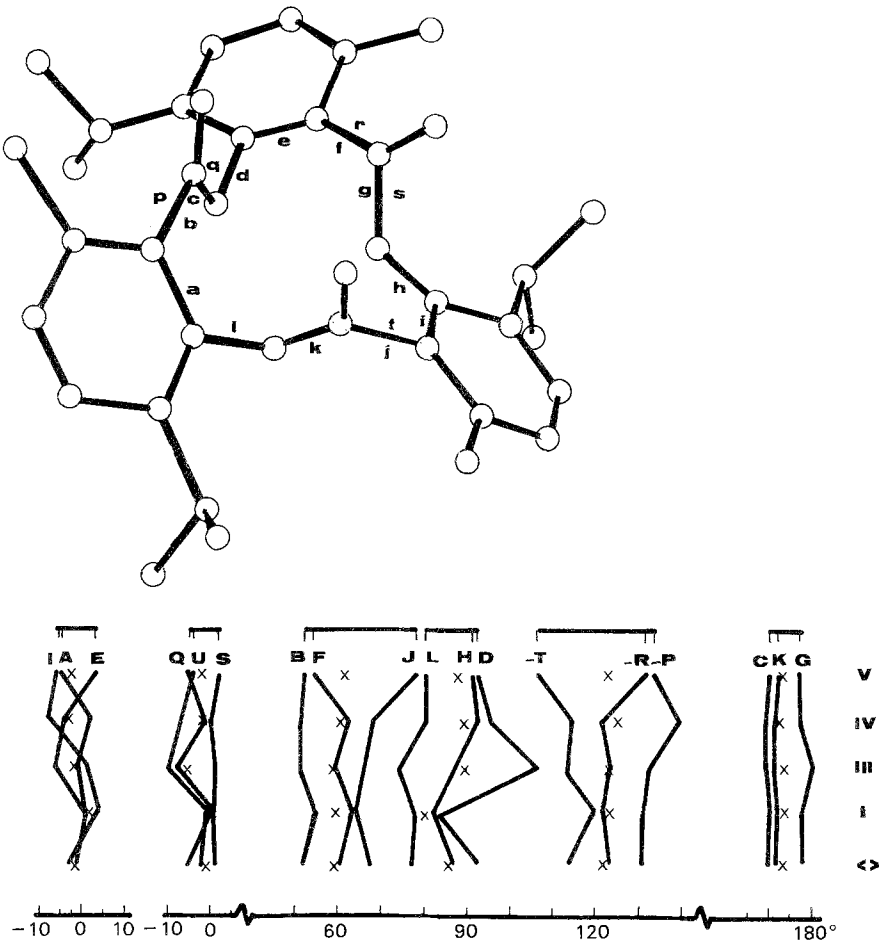

I *trans*-stilbene complex (molecule I of [16])
III unsolvated TOT
IV *n*-cetyl alcohol complex
V ethanol complex
x average of the three equivalent parameters for each compound
<> average of I, III, IV and V

Fig. 2. Torsion angles of TOT in different crystalline environments.

group $P3_121$ clathrates formed with guest molecules **2**, **10**, and **11**, the maximum difference of atomic coordinates is 0.15 Å; the mean difference is 0.04 Å. Similar observations hold for *cis*- and *trans*-stilbene $P\bar{1}$ clathrates.

3. Chiral Discrimination

In its guest-free form, TOT is a racemic compound crystallizing in the achiral space group $Pna2_1$ [18]. But in the presence of solvent molecules of appropriate size, acting as potential guests, new phenomena appear [4,5,13,19,20]:

– In the presence of optically pure solvent, optically pure TOT clathrates are obtained belonging to the $P3_121$ cage type: thanks to the rapid *P–M* interconversion of TOT, the guest chirality imposes itself on the whole clathrate, i.e. a given configuration of guest always leads to single crystals or powder containing the same configuration of TOT.

– In the presence of a racemic solvent, TOT undergoes spontaneous resolution and a conglomerate is obtained. Each single crystal of space group $P3_121$ contains TOT of the same chirality, but it includes both guest enantiomers, the enantiomeric excess (e.e.) varying for different 'host lattice/guest molecule' combinations (Table III). Separation and identification of these crystals as (+)- or (–)-TOT can be achieved by taking a chip from each crystal, and then measuring its rotation in solution.

Table III. Enantiomeric excess of guest and correlation of guest and host chirality in *P*-(+)-TOT clathrate crystals

	Guest	Clathrate type	Guest ee, % [13,19]	Guest ee, % [15]	Guest config.
1	2-chlorobutane	cage	32	45	*S*-(+)
2	2-bromobutane	cage	37	35	*S*-(+)
3	2-iodobutane	cage	< 1		
4	2-chlorooctane	channel	4		*S*-(+)
5	2-bromooctane	channel	4		*S*-(+)
6	3-bromooctane	channel	4		*S*-(+)
7	2-bromononane	channel	5		*S*-(+)
8	2-bromododecane	channel	5		*S*-(+)
9	*trans*-2,3-dimethyloxirane	cage	47		*S, S*-(–)
10	*trans*-2,3-dimethylthiirane	cage	30		*S, S*-(–)
11	*trans*-2,4-dimethyloxetane	cage	38		
12	*trans*-2,4-dimethylthietane	cage	9		
13	propylene oxide	cage	5		*R*-(+)
14	2-methyltetrahydrofuran	cage	2		*S*-(+)
15	methyl methanesulfinate	cage	14		*R*-(+)
16	2,3,3-trimethyloxaziridine	cage	7		
17	ethyl methyl sulfoxide	cage		40–50	*R*-(+)
18	2-butanol	cage		< 5	*S*-(+)
19	2-aminobutane	cage		< 2	

Remark. The data in Table III represent the enantiomeric excess in crystal grown from a *racemic solution* of guest. But enantiomeric discrimination can be considerably enhanced when optically active solutions of guests are used; this results in amplification of guest optical purity after repeated crystallizations. For instance, after 3 cycles, the enantiomeric purity of **5** reaches 80% [13], despite the very low enantiomeric purity (4%) resulting from the first crystallization.

Powell first pointed out that TOT enclathration might be used to establish the absolute configuration of guests. The *absolute configuration* of TOT has been assigned by determining the configuration of TOT relative to guest, for several guest molecules of known absolute configuration: (+)-TOT has a *P*-propeller like configuration [20,21]. Conversely, now, the absolute configuration of new guest molecules can be determined by X-ray analysis of TOT

clathrates. But even without such an analysis a reasonable inference can be made about the absolute configuration of the preferred guest enantiomer. Indeed it has been noted that homologous atoms or groups of atoms in related molecules occupy similar positions in space (Figure 3). The combined measurement of TOT and guest optical rotation would then lead to the determination of the absolute configuration of the guest [13].

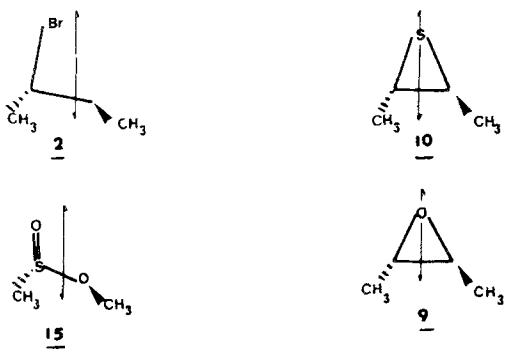

Fig. 3. Enantiomers of guest molecules **2**, **9**, **10** and **15**, which are preferentially included in a clathrate crystal built of P-(+)-TOT molecules. The guests are presented in the orientations that they adopt relative to the 2-fold axis of the cage cavity.

Assignments of absolute configuration by means of TOT structures rely on the hypothesis that the correlation of the absolute configurations of the host and the preferred guest enantiomer is an intrinsic property of the complex and remains unchanged in every single crystal of a given clathrate. As one test of this hypothesis, an attempt has been made to grow TOT clathrates containing an excess of 'unnatural' enantiomer, (+)-TOT. (+)-(*R*, *R*)-**9**. Single crystals containing (+)-TOT were used to seed saturated solutions of TOT in (+)-(*R*, *R*)-**9**. The (+)-TOT seed might have continued to grow and incorporate (+)-TOT and the only available guest, (+)-(*R*, *R*)-**9**. However, the seed crystals failed to grow, and a powder of clathrate crystals precipitated, comprised of a complex of chirality opposite to that of the seed crystals. This result implies that formation of inclusion complexes with an intrinsically less favorable guest enantiomer as the sole included species is not possible, at least for a guest for which chiral discrimination is substantial. In cases where discrimination is very weak, perhaps both complexes may be observed.

The *enantiomeric excess (e.e.)* of guest depends on several factors:

- Discrimination in *channels* is considerably weaker than in *cages*, presumably as a result of increased disorder.
- Coincidence between *cage symmetry* (two-fold axis) and guest *molecular symmetry* could be expected to be a favorable factor. Indeed, **9–12** tend to afford high e.e. We note however the high discrimination of **1** and **2**, although both lack two-fold symmetry.
- The size of the guest is an important factor: the smallest (**13**) and largest (**14**) molecules of the series **9–16** exibit the least e.e.
- Conversely, *chemical functions* like —OH or $-NH_2$ do not seem to lead to a favorable effect (a discussion based on semiempirical calculations is found in [15]).

3.1. STRUCTURAL DATA. INTERPRETATION OF CHIRAL DISCRIMINATION

The cages are located on a crystallographic 2-fold axis; Their centers are separated by about 13 Å. Each cavity is comprised of eight TOT molecules; six form a cylindrical wall that is approximately parallel to the *c* axis; one molecule is on top and one on the bottom (looking at the cage along the *c* axis).

X-ray analysis of several compounds revealed unexpected facts. The cage (Figure 4) appears as a deformed ellipsoid and its capacity for enantiomeric discrimination is not obvious; even less so is the prediction of the configuration of the preferentially included guest.

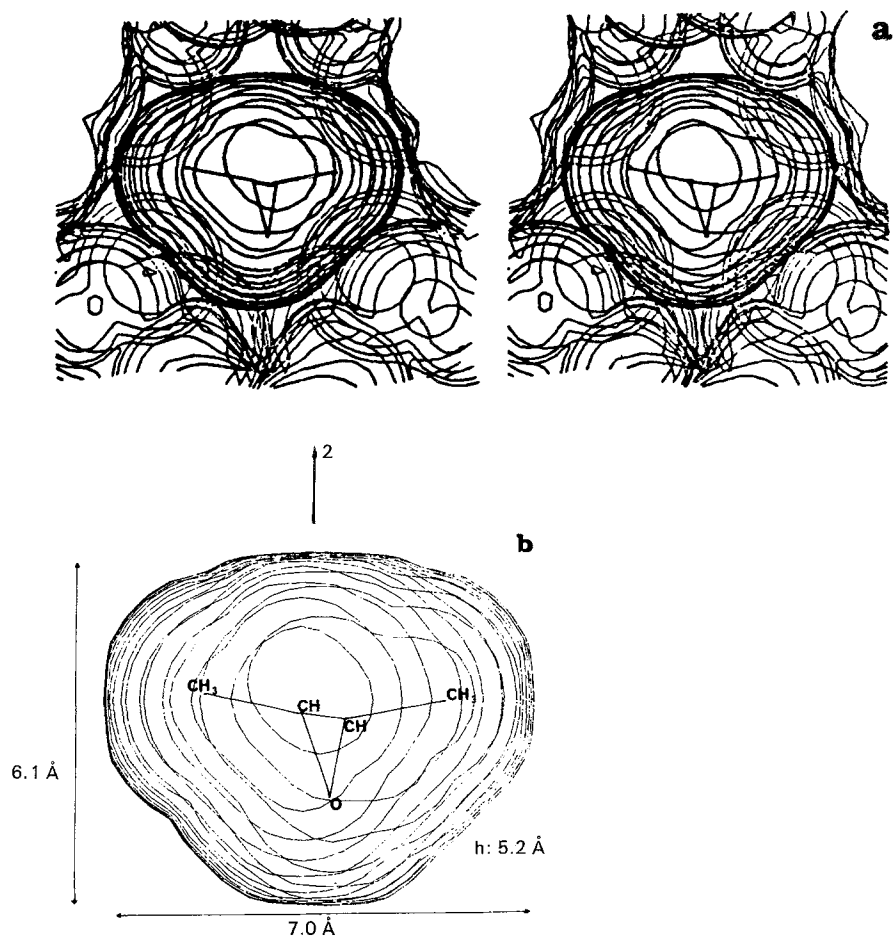

Fig. 4. (a) Stereoview of the contours of the van der Waals envelope of TOT (light lines) and of the van der Waals envelope of the volume accessible to guest atoms, (heavy lines), viewed along the *c* axis. Sections are plotted every 0.3 Å, parrallel to the *ab* plane, in a cube having 9.2 Å sides and centered on (0, 0.33, 0.1667). The position of (+)-(*R*, *R*)-2, 3-dimethyloxirane is shown. (b) Dimensions of the van der Waals envelope of the space available to the guest; sections and guest are drawn as in (a).

Moreover, a general characteristic of cage clathrate structures is the presence of different kinds of disorder:

(a) *Enantiomeric disorder*: naturally present in crystals grown from racemic solution.

(b) *Crystal symmetry disorder*: this also could be expected for guests lacking two-fold symmetry. Figure 5 shows four superimposed positions corresponding to both disorders (a) and (b).

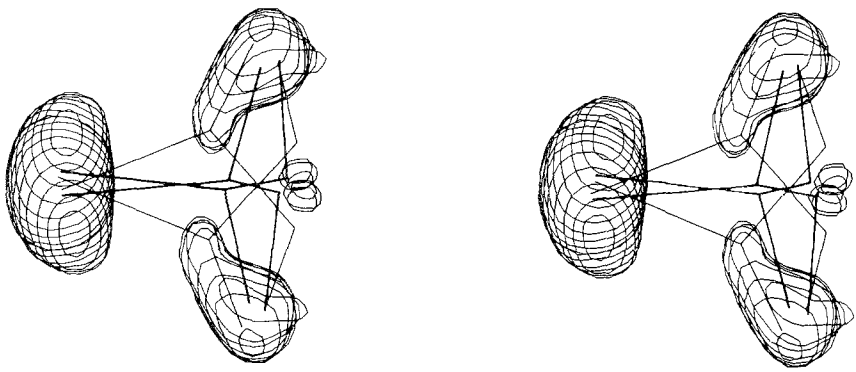

Fig. 5. Electron density distribution of 2-bromobutane in its average position of two-fold disorder in a cage framework consisting of (M)-TOT molecules (calculated from a Fourier synthesis). The contours include about 90% of the total electron population. Heavy line: *R* configuration of the X-ray model. Thin line: calulated position of the *S* enantiomer (from [12]).

More unexpectedly, even for optically pure **9** and **10**, two symmetry-related positions are located within the cage; however these positions are not very far from the special positions (a few tenths of an Å). The methyl group and the heteroatoms of these two disordered molecules occupy fairly close positions and the disorder concerns mainly the carbon ring atoms. It is worth emphasizing that chiral discrimination occurs despite the observed disorder.

The determination of the atomic positions of the guest, in all cases of disorder, is not an easy task. It is then appropriate to cite some technical details. In the crystal structure determination of the TOT-**2** clathrate at 223 K, the final *R* factor for 2714 observed nonzero intensity reflections is 0.076 [13]. An independent determination [12] at 125 K with 2286 reflections led to $R = 0.081$; the possibility of a slight pseudosymmetry, assuming space group $P3_1$, is evoked in this reference. We note finally that the *R* factor for optically pure **9** (6.4%) and **10** (8.3%) clathrates are also in the same range.

In conclusion, the picture of host/guest interactions does not provide an immediate clue to the ultimate mechanism of chiral discrimination, which seems to result from an overall interaction rather than a precise 'three point model'. In addition to the static geometry, dynamical considerations may be involved. The 'rigidity' of the cage walls, intuitively an important factor in chiral discrimination, cannot be easily appreciated. The temperature dependance of physical phenomena may provide an indication about the cage rigidity. Indeed, a relevant fact is provided by racemization of **15** within the cage: crystals heated to 115°C for up to 12 hours showed no racemization, whereas in solution complete racemization takes place at that temperature. However, on heating the crystals at 125°C for 12 h, racemization proceeded and the enantiomeric purity falls to zero. This clearly shows that increased thermal movements of the TOT atoms at the cage internal surface result in the loss of the chiral discrimination ability of the clathrate above a certain temperature. The influence of thermal factors on a different kind of phenomenon, photoisomerization, is described in the next section.

4. Photoisomerization of Guest Molecules

Enantiomeric separation is still a physical phenomenon governed essentially by molecular interactions in the crystal state. The sulfinate racemization experiment mentioned above may be considered as a first step towards the study of chemical reactions. Photoisomerization of olefin derivatives has been the subject of detailed work.

The essential facts can be summarized by the following scheme:

	solution	TOT-clathrate	pure guest crystal
	cis ⇌ *trans*	*cis* → *trans*	*cis* ↛ *trans*
stilbenes	80% 20%	*cis* ↚ *trans*	*cis* ↚ *trans*
	cis ⇌ *trans*	*cis* ⇌ *trans*	*cis* ← *trans*
cinnamates	50% 50%	50% 50%	*cis* ↛ trans

The scheme is valid for the majority of derivatives tested.

In both types of guest molecules, stilbenes and cinnamates, the *cis–trans* isomerization pattern in the clathrate is different from that observed in pure guest crystals. This is ascribed, generally, to specific host–guest interactions, totally different from the guest–guest interaction occuring in the pure guest crystal. Furthermore, cinnamates, but not stilbenes, show the same behaviour in clathrates as is observed in solution. An interpretation of the facts requires combined crystallographic and chemical studies.

All clathrates crystallize in $P\bar{1}$ with two (2TOT · guest) units per unit cell. Both crystal structures of the *cis*- and *trans*-stilbene have been determined and refined ($\sim$ 7700 independant reflections for the *trans*, 5300 for the *cis*) [16]. A recent publication [17] describes the structure of a clathrate with benzene, isomorphous to the stilbene clathrate. Benzene was one of the first achiral molecules shown to form a $P3_121$ clathrate [4]. We have here a case where the adopted crystal structure of the clathrate depends on experimental conditions.

The location of the guest molecules within the cavity system deserves a special description for each guest.

Trans-stilbene – One molecule is located at (0, 1/2, 0) within a 'channel' running along *a*; the other, at (1/2, 1/2, 1/2) within a 'channel' running along *b* (Figure 6a). But these channels display a markedly variable section and shape, as is shown in Figure 7. This geometrical pattern could also be described as cavities interconnected by thin channels. The stilbene molecules are clearly located on a difference Fourier map; their temperature factor is higher than those of the matrix, denote a very slight orientational disorder (statistical or dynamical).

Cis-stilbene – The guest molecules could not be located. It is worth noting that their global occupancy factor is less than 1. But the shape of the channels in the *trans*-stilbene clathrate may provide some indications. In the *a* channel a 'pocket' visible near the center of symmetry (0, 1/2, 0), can accomodate one of the benzene rings of *cis*-stilbene; the other ring may occupy a space near the same position as one of those of *trans*-stilbene, centered at (0.72, 0.46, 0.95).

In the *b* channel, the accessible space around (1/2, 1/2, 1/2) seems 'tailored' for *trans*-stilbene, and no room for another benzene ring is left at that location. But there is room at the ends of *trans*-stilbene (Figure 7); a tentative location of one benzene ring is near (1/2, 0, 1/2). Another possibility, at (0, 0, 1/2) emerges below from the study of the benzene clathrate.

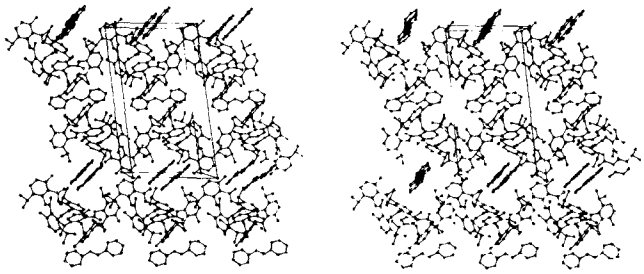

Fig. 6a. Stereoscopic drawing, made with ORTEP, of the *trans*-stilbene. TOT clathrate structure viewed along the x axis. The axial directions are a out of the plane of the paper, $b \rightarrow$, and $c \uparrow$.

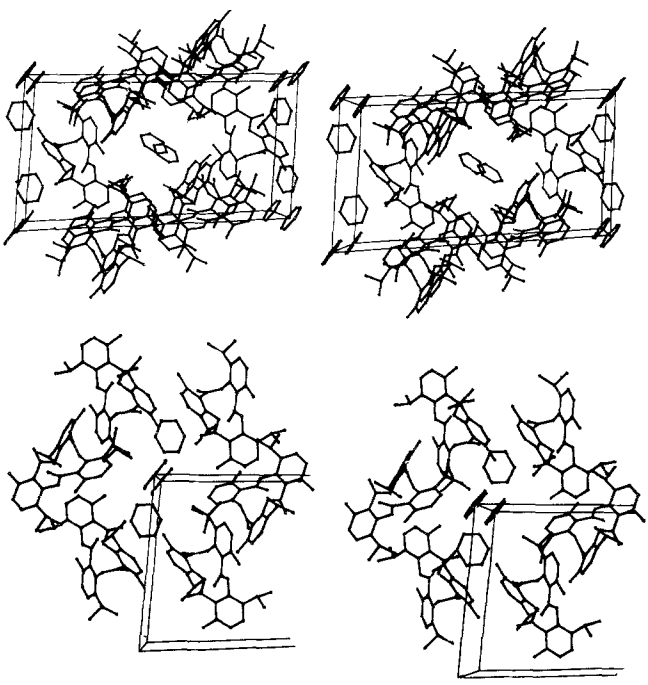

Fig. 6b. Stereoscopic view of the packing of the benzene clathrate along the a axis. The origin is at top left, a is directly towards observer, b from up to down and c from left to right. The origin in this clathrate corresponds to (0, 0, 1/2) of the *trans*-stilbene clathrate (from [17]).

Benzene – The structure contains three independent ordered molecules, but their occupancy factors are significantly smaller than 1 (Figure 6b). A remarkable feature is the nearly perfect coincidence between the location of four benzene molecules in the unit cell of this clathrate (occupancy 0.8) and that of the benzene rings in the *trans*-stilbene clathrate: two molecules around (0, 1/2, 0) in the a channel, two molecules around (1/2, 1/2, 1/2) in the b channel. There is an additional benzene molecule located at (0, 0, 1/2) (occupancy 0.4), located at the intersection of the b channel and a third channel, directed along a. This may give a new clue to the actual position of *cis*-stilbene in the TOT clathrate, since a new potential site for a benzene ring is described.

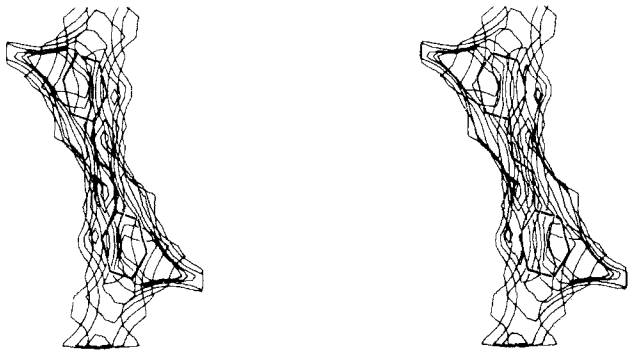

Fig. 7. Stereoscopic drawing of cavity enclosing the *trans*-stilbene (centered on (1/2, 1/2, 1/2)) in the channel parallel to the *b* axis. The contours of the volume accessible to the stilbene atoms are drawn in sections separated by 0.4 Å and parallel to the (a, b) sections plane; they are viewed normal to the (a, b) plane and are included in a parallelepiped defined by $0.24 \leqslant x \leqslant 0.76$, $0 \leqslant y \leqslant 1$, $0.38 \leqslant z \leqslant 0.62$. A point is considered as accessible to stilbene atoms if its distance to the van der Waals envelope of TOT is larger than 1.5 Å.

The crystal structures provide a simple and important clue for understanding the unidirectional *cis–trans* conversion: the coincidence between the *molecular symmetry* of *trans*-stilbene and the *symmetry of the crystallographic site* at which the guest molecule is located. *Cis*-stilbene lacking a $\bar{1}$ symmetry is necessarily disordered in $P\bar{1}$. It follows that it is impossible for this clathrate to 'optimize' the host/guest contacts simultaneously for both moieties, and we can reasonably infer a considerably larger thermodynamic stability of the *trans*- over the *cis*- stilbene clathrate. By contrast, both *cis*- and *trans*-methyl cinnamate lack $\bar{1}$ symmetry; in addition, they are smaller than the stilbenes. These facts may account for the observed photoequilibrium, identical to that observed in solution (Figure 8), whether one starts from the *cis*- or from the *trans*-cinnamate clathrate.

Next, we consider the *mechanism* of the *cis* → *trans* isomerization within the *cis*-stilbene clathrate. Whatever the location of the guest, among those described above, inspection of the

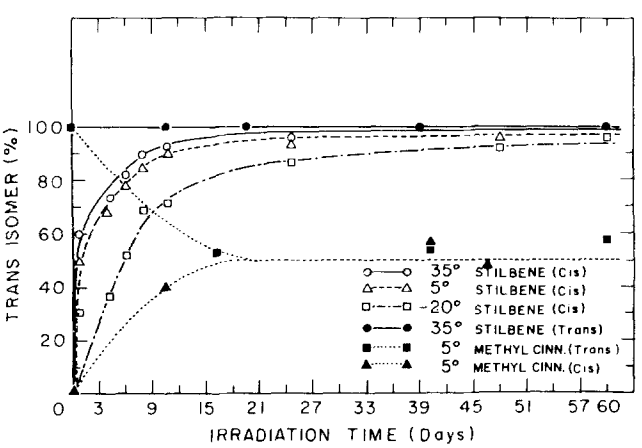

Fig. 8. Irradiation of TOT clathrates of *cis*-(▲) and *trans*-(■) methyl cinnamate and *cis*-(○) and *trans*-(●) stilbene. For the irradiation of powdered samples of *cis*-stilbene. TOT clathrate as a function of temperature, the starting samples were taken from the same batch of clathrate. Analyses were performed by gas chromatography and the ratios were calibrated against known mixtures of *cis* and *trans* isomers; limits of error ± 10%. The phenanthrene formed from the *cis*-stilbene clathrate has not been included.

crystal structure shows that there is no room to allow the intramolecular rotation to take place inside the channel. A possible explanation resides in the 'loosening' of the surrounding TOT structure, coinciding with the absorption of a photon by stilbene. The TOT molecules would then undergo a concerted movement so as to allow both the intramolecular *cis–trans* rotation and the necessary displacement of the newly formed *trans*-stilbene molecules towards the final ordered position in the corresponding clathrate. This amounts to a local destruction, or at least severe deformation, of the *cis*-stilbene clathrate structure and subsequent 'recrystallization' in the *trans*-stilbene clathrate structure. This mechanism accounts for the fact that the initial single crystal is destroyed to yield an aggregate of crystallites in the product phase.

The necessary activation energy being of thermal origin, the kinetic study of the phenomenon is of interest. Indeed, the temperature dependance of the isomerization kinetics must probably reflect the thermal barrier for the above rearrangement of the TOT structure (Figure 8). We note that no such temperature dependance occurs for the isomerization of free *cis*-stilbene. Furthermore, it has been shown that iodine catalyses, in the dark, the *cis–trans* conversion in the clathrate. But the iodine promoted conversion is completely inhibited at $-20°C$ (whereas for free *cis*-stilbene it is only retarded at $-20°C$). These facts again reflect the thermal barrier for the penetration of iodine through the TOT lattice. They favour an *in situ* isomerization, within the cavities, and not in interstitial pockets such as dislocations or other defects.

5. Isolation of Monomeric Carboxylic Acids

The ease with which TOT clathrates are formed reflects the pronounced stability of the clathrate structure over the separate crystal structures of guest and host species. One could then further inquire about the ability of the clathrate to displace an equilibrium due to strong guest–guest interactions. A well-known example of such strong interaction is that of carboxylic acids, which display the well-known, hydrogen-bonded dimeric form in the crystal state, in solution, in the liquid state, and even in the gas state. Indeed, clathrates are ideal media for matrix isolation at room temperature. Otherwise, it was only by laborious argon or nitrogen matrix isolation techniques at 4 K that pure monomeric IR spectra of carboxylic acids were recorded. The isolation of monomeric acetic acid in Dianin's compound inclusion complexes has been reported, although other possibilities could not be ruled out, since there were 2 *guest molecules per cage* in the complex crystal. The isolation of monomeric acetic and propionic acid (see also p. 275 of this issue) [22] within the cages of $P3_121$ TOT clathrate has been recently performed [23]. The cage-type clathrates reveal *sharp peaks at* 3475–3445 cm^{-1} which disappear when the crystals are dissolved in chloroform, while the spectra of the channel-type acid complexes display wide bands extending from 3400 to 2300 cm^{-1}. These peaks are characteristic, respectively, of free OH bonds and strong OH···O hydrogen bonds.

The crystal structure determination of the acetic acid clathrate confirms the monomeric inclusion, and reveals further that only van der Waals host/guest contacts are present. No hydrogen bond is formed between the guest and TOT oxygens. Besides the intrinsic interest of matrix isolation, the above study provides additional striking evidence for the importance of residual forces in crystal structure engineering. A further illustration arises from the fact that there is no disorder resulting from the exchange of the carbonyl oxygen and the methyl-group of the acetic acid. Even in the absence of a hydrogen bond, the TOT cage still discriminates perfectly between these two groups, Similarly, in the 2-bromobutane clathrate, there is no disorder from exchange of Br with CH_3 despite their almost identical van der Waals envelopes.

6. Summary and Perspective

The ability of TOT to form clathrates is characterized by an unusually large number of crystalline forms. At least ten different space groups have been identified. Three forms have been thoroughly investigated; for one of them, the cage-type $P3_121$, nine independent crystal structure determinations have been accomplished. This wealth of structural data greatly contributes to the interpretation of various physicochemical phenomena specifically arising from host/guest interactions.

In the chirality domain, the predictions of Powell have been amply confirmed by determining a significant and often large (up to 2/3) enantiomeric excess for enclathrated guests. For practical applications, the optical purity of the guest recovered from the first crystallization of the clathrate can be further enhanced to nearly 100% by repeated crystallization. A quite unexpected fact requires particular attention: the disorder of guest molecules does not always prevent chiral discrimination. A definite interpretation of chiral discrimination on the basis of the geometrical and chemical nature of the cage is not yet clear.

New work is called for in this area: a more detailed analysis of host/guest interactions, possibly by 'molecular mechanics', and quantum mechanics models; experiments with other molecules of different shape and chemical functions; further investigations of the channel clathrates to assign the nature of guest disorder (head-to-head, head-to-tail, or random arrangement of the guests): investigation of the $P2_1$ clathrates; asymmetric synthesis within the cages. In this connection a recent communication [24] has reported the following asymmetric reaction within the cage of a $P3_121$ clathrate:

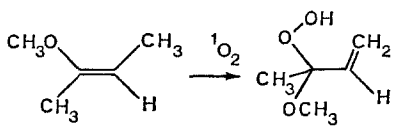

Another domain of cage controlled reactions is provided by the *cis–trans* isomerization of olefins: the reaction pathway is different from that occurring in solution or from that in the pure guest crystal. It is believed that the most important fact governing these reactions is the relation between the crystallographic and the molecular symmetry. Common characteristics with the chiral discrimination problem are found: the role of symmetry, the role of disorder, the role of TOT flexibility. The isolation of carboxylic acid monomers further illustrates the strength of cage/guest interactions.

It appears now that in the course of investigations on new physicochemical phenomena, TOT clathrates offer a great range of possibilities.

References

1. G. Naquet: *Bull. Soc. Chim. Fr.* **4**, 93 (1865).
   R. Spallino and G. Provenzal: *Gazz. Chim. Ital.* **39**, 11 (1909).
2. W. Baker, B. Gilbert and W. D. Ollis: *J. Chem. Soc.*, 1443 (1952).
3. A. C. D. Newman and H. M. Powell: *J. Chem. Soc.*, 3747 (1952).
4. D. Lawton and H. M. Powell: *J. Chem. Soc.*, 2339 (1958).
5. H. M. Powell: *Nature (London)* **170**, 155 (1952).
6. H. M. Powell: *Endeavour* **15**, 20 (1956).
7. R. Popovitz-Biro, C. P. Tang, H. C. Chang, N. Shocher, M. Lahav and L. Leiserowitz: *Nouv. J. Chim.* **6**, 75 (1982).

8. A. P. Downing, W. D. Ollis and I. O. Sutherland: *J. Chem. Soc. B.*, 24 (1970).
9. W. D. Ollis, J. A. Price, J. Stephanidou Stephanatou and J. F. Stoddart: *Angew. Chem. Int. Ed. Engl.* **14**, 169 (1975).
10. D. J. Williams and D. Lawton: *Tetrahedron Lett.*, 111 (1975).
11. S. Brunie, A. Navaza, G. Tsoucaris, J. P. Declercq and G. Germain: *Acta Crystallogr.* **B33**, 2645 (1977).
12. J. Allemand and R. Gerdil: *Acta Crystallogr.* **B38**, 1473 (1982).
13. R. Arad-Yellin, B. S. Green, M. Knossow and G. Tsoucaris: *J. Am. Chem. Soc.* **105**, 4561 (1983).
14. J. Allemand and R. Gerdil: *Acta Crystallogr.* **B38**, 2312. (1982).
15. R. Gerdil and J. Allemand: *Helv. Chim. Acta* **63**, 1750 (1980).
16. R. Arad-Yellin, S. Brunie, B. S. Green, M. Knossow and G. Tsoucaris: *J. Am. Chem. Soc.* **101**, 7529 (1979).
17. J. Allemand and R. Gerdil: *Acta Crystallogr.* **C39**, 260 (1983).
18. S. Brunie and G. Tsoucaris: *Cryst. Struct. Commun.* **3**, 481 (1974).
19. R. Arad-Yellin, B. S. Green and M. Knossow: *J. Am. Chem. Soc.* **102**, 1157 (1980).
20. R. Gerdil and J. Allemand: *Tetrahedron Lett.*, 3499 (1979).
21. R. Arad-Yellin, B. S. Green, M. Knossow and G. Tsoucaris: *Tetrahedron Lett.* **21**, 387 (1980).
22. J. E. D. Davies: *J. Incl. Phenom.* **3**, 269 (1985).
23. R. Arad-Yellin, B. S. Green, M. Knossow and N. Rysanek: to be published.
24. R. Gerdil, G. Barchietto and C. W. Jefford: *IIIMIP. IICD*, Tokyo, Japan (1984).